Article

Journal of
Nanoscience and Nanotechnology
Vol. 18, 4805–4813, 2018
www.aspbs.com/jnn

Direct Electrochemistry of Methanobactin Functionalized Gold Nanoparticles on Au Electrode

Jiaying Xin[1, 2, *], Boxin Dou[1], Zhenxing Wang[1], Yan Wang[1], Chungu Xia[2], and Zhongfan Liu[3]

[1] *Key Laboratory for Food Science and Engineering, Harbin University of Commerce, Harbin 150076, Heilongjiang Province, China*
[2] *State Key Laboratory for Oxo Synthesis and Selective Oxidation, Lanzhou Institute of Chemical Physics, Chinese Academy of Sciences, Lanzhou 730000, Gansu Province, China*
[3] *Chemistry College of Beijing University, Beijing 100871, China*

Mathanobatins (Mb, Mbtins) were immobilized successfully on nanometer-sized gold colloid particles associated with β-mercaptoethylamine. The structures of Mb functionalized gold nanoparticles were characterized and confirmed by UV-vis spectroscopy (UV-vis), FTIR spectra and electrochemical analyses. Direct electron transfer between Mb or copper-loading Mbtins and the modified electrode was investigated without the aid of any electron mediator. The copper-loading Mbtins act as a better electrocatalyst for the reduction of H_2O_2 than Mb. The copper-loading Mb, with which gold nanoparticles were functionalized, as a model enzyme, was immobilized on gold electrode to construct a novel H_2O_2 biosensor. In pH 6.4 phosphate buffer solution, the reduction and oxidation peak potentials of Mb functionalized gold nanoparticles modified Au electrode (copper-loading Mbtins) were 0.115 and 0.222 V. On the surface, capacitance per unite area (C_d) of Mb functionalized gold nanoparticles modified electrode were 38 μF cm^{-2}. The immobilized Mb displayed the features of a peroxidase and gave an excellent electrocatalytic response to the reduction of H_2O_2. The detection limit of Mb functionalized gold nanoparticles (copper-loading) were 09×10^{-5} mA/M ($S/N = 3$). The Michaelis–Menten constant (Km) was 0.787 mM. Good stability and sensitivity were assessed for the biosensor.

Keywords: Methanobactin, Direct Electrochemistry, Gold Nanoparticles, Self-Assembled Monolayer, Hydrogen Peroxide.

1. INTRODUCTION

To capture enough Cu^{2+}, Methanotroph (such as Methylosinus trichosporium OB3b, Methylococcus capsulatus) secrete a kind of mimic peptides, which is Methanobactin (Mb, Mbtin). Mb has the abilities to capture Cu^{2+} outside the cell and transfer captured Cu^{2+} into the cell, activate the expression of pMMO, and help Methanotroph to stimulate catabolism of methane. In our previous work, we have reported loaded copper Mb had a good ability for reduction.[1–3]

Of interest is that Mb is not specific for copper only, but also reduce Au(III) to Au(0) used in synthesis of gold nanoparticle. The monodispersity gold nanoparticles modified Mb were successfully produced.[1, 4, 5] At the same time, the Mb still keeps its biological activity.

Generally speaking, the size of protein focuses on nanometer scale, the nanomaterials are suitable for proteins and easier to open the active center. The reason may be that the nanometer-sized gold colloids immobilized on active materials (such as the redox peptides and enzymes) play an important role similarly to a conducting wire or electron-conducting tunnel, which makes them easier for the electron transfer to take place.[6]

Electrochemistry is a new means for researching phenomenon of life science. Electronic exchange between proteins in solution or adsorbed on surface of electrode directly and electrode take place, this interaction, in a way, is similar to electron transfer between proteins and biofilms within organisms. In recent years, the applications of nanometer gold to simulate the biosensor of peroxidase have been reported.[7–12]

In this study, we studied how to use thiol-tailed or amine groups of β-mercaptoethylamine to prepare Mb

*Author to whom correspondence should be addressed.

functionalized gold nanoparticles which were immobilized on bare gold electrode and displayed much better monolayer through self-assembly, firstly. The biological activities and structure of Mb were characterized with UV-vis spectroscopy, fluorescence spectroscopy and FTIR spectra. Then, electrochemical impedance spectroscopy (EIS) and cyclic voltammograms (CV) were used to characterize the modified process of bare gold electrodes. Finally, the copper ions were coordinated at the surface of the modified electrode which response to the reduction of H_2O_2 was studied.

2. MATERIALS AND METHODS

2.1. Chemicals

Methanobactin (Mb) from the spent medium of *Methylosinus trichosporium* 3011, which was obtained from the Institute of Microbiology and Virology (Kiev, Ukraine), was grown up in a 5 L bioreactor containing 3 L copper-deficient nitrate minimal salts (NMS) medium as previously described.[13] β-mercaptoethylamine was purchased from Sigma. $AuCl_3HCl{\cdot}4H_2O$ (Au% > 48%, the Shanghai No. 1 Reagent Factory) and all other chemicals were of analytical grade. Phosphate buffer solutions (0.02 M) with various pH values were prepared by mixing stock standard solutions of Na_2HPO_4 and NaH_2PO_4 and adjusting the pH with 0.1 M H_3PO_4 or NaOH. All solutions were made up with twice-distilled water.

2.2. Apparatus and Methods

The UV-vis reflection and absorption spectra were recorded with a Shimadzu UV-2550 spectrophotometer (Japan). The FTIR spectra of Mb, Mb-AuNPs nanocomposite, Mb functionalized gold nanoparticles and modified gold nanoparticles were measured using an F-7000 Fourier transform infrared (FTIR) spectrophotometer (HITACHI, Japan). Samples for the FTIR were prepared by freeze-dried Mb, Mb-AuNPs and the MB functionalized gold nanoparticles for powder diffraction measurements. The samples were dried and ground with KBr to prepared KBr pellets and analyzed by PerkinElmer 100 operating at a resolution of 4 cm^{-1} over 4000–450 cm^{-1}.

All electrochemical measurements were performed at a CHI630 electrochemistry work station (Shanghai Chenhua Co., China). The electrochemical cell consisted of a three-electrode system where the modified gold electrode (3 mm in diameter, Shanghai Chenghua, China) was used as the working electrode. The reference electrode was an Ag/AgCl electrode CHI111 (Shanghai Chenhua Co., China). The counter electrode was a platinum wire (99% pure). All measurements were carried out at a temperature of 25 ± 0.2 °C in a Faraday cage. The Mb used in this study was found to be stable to repeated scanning and rinsing of the electrode, therefore it was concluded that it was adsorbed strongly to gold. The pH value was measured with a pH meter purchased from Hanna Instruments (Model 210). All glassware used in the following procedures was cleaned in a bath of freshly prepared 3:1 $HNO_3 + HCl$, rinsed thoroughly in twice-distilled water and dried in air.

2.3. Preparation of Mb Functionalized Gold Nanoparticles

The Mb was prepared and purified according to the Ref. [14], the concentration was 0.025 M. And then Mb-AuNPs were prepared by biological synthesis method,[3] the concentration was 0.025 M, too. According to the image analysis performed on a TEM micrograph, the obtained AuNPs were predominantly spherical with an average size of 19.3 ± 5.5 nm.

The Mb functionalized gold nanoparticles were prepared as follows: Firstly, pure gold nanoparticles were prepared by Frens method.[15] The solution was quickly turned into a ruby-red solution, indicating the formation of the AuNPs. Then, 5 μL of 0.05 M β-mercaptoethylamine aqueous solution was added into the 2 mL of AuNPs aqueous solution preserved 24 hours at 4 °C. The mercaptoethylamine-AuNPs were achieved. Finally, Mb solution was added into the 2 mL of functionalized gold nanoparticles aqueous solution (mole ratio was 1:1) to prepare Mb functionalized gold nanoparticles. All samples were stored in the dark. The resulting nanocomposite was used for all the characterizations and experiments. Such a nanocomposite was stable in water even after 3 months storage.

2.4. Electrode Modification and Electrochemical Measurements

The gold electrodes were firstly polished with abrasive paper and then with alumina (0.25 and 0.05 μm) slurry on microcloth pads, followed by rinsing with water and ethanol and briefly cleaning in an ultrasonic bath.

The surfaces of cleaned gold electrodes were respectively modified by adding 20 μL of Mb, Mb-AuNPs, mercaptoethylamine-AuNPs and Mb functionalized gold nanoparticles aqueous solution for 16 h at 4 °C in darkness. The resulting monolayer-modified electrode was rinsed thoroughly with twice-distilled water. However, the gold colloid- mercaptoethylamine-modified gold electrode was also added the Mb solution on the surface for 10 h at 4 °C. In such a way, the Mb-modified gold electrode, Mb-AuNPs-modified gold electrode, Mb-AUNPs-mercaptoethylamine modified gold electrode and Mb functionalized gold nanoparticle modified gold electrode were obtained. All resulting electrodes were washed with water and stored in pH 7.0 PBS at 4 °C. One hand, the association of Mb with the AuNPs surface occurs due to the interaction between SH^- or NH_4^+-lysine residues of Mb and the gold colloid surface. On the other hand, it occurs due to the interaction between –SH and $–NH_2$ of β-mercaptoethylamine and the gold colloid surface.

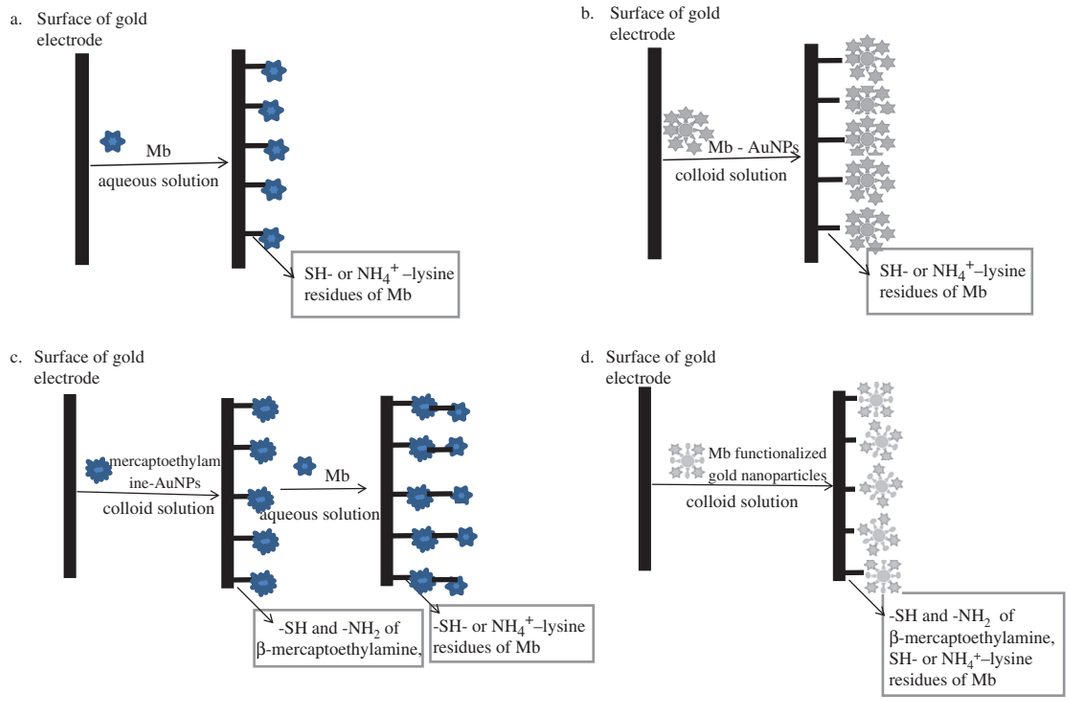

Scheme 1. Preparation process of the modified gold electrodes. (a) Mb-modified gold electrode; (b) Mb-AuNPs-modified gold electrode; (c) Mb-AUNPs-mercaptoethylamine modified gold electrode; (d) Mb functionalized gold nanoparticles modified gold electrode.

The preparation process of the modified electrodes is shown in Scheme 1. Then all above modified gold electrodes were immersed in 0.1 M $CuSO_4$ solution for 20 h, at 4 °C. After coordination with copper ions, the modified electrodes were also measured by electrochemical measurements.

The electrochemical impedance spectroscopy (EIS) was obtained by using 0.1 M KCl solution containing 5.00×10^{-3} M $K_3[Fe(CN)_6]$ and 5.00×10^{-3} M $K_4[Fe(CN)_6]$. All the cyclic voltammetry experiments of Mb with loaded copper were carried out in 7 mL of 0.02 M (pH value was 6.4) phosphate buffer saline (PBS) solution, and the solution was purged with high purity nitrogen prior to and blanked with nitrogen during the electrochemical experiments. Amperometric experiments were carried out in a stirred system by applying a potential step of −200 mV to the working electrode.

3. RESULTS AND DISCUSSION

3.1. UV-Vis Reflection Spectroscopy (UV-Vis)

The UV-vis spectrum of Mb solution showed Soret bands at 280 nm, 340 nm and 395 nm in pH 7.0 PBS (Fig. 1). The wavelength of pure Au nanoparticles was 530 nm (Fig. 1(a)). The locations of the Soret absorption band of Tyr residues, oxazolone and imidazolone may provide information about the Mb. When Mb was denatured, the Soret band shifted or disappeared.[1,2] As shown in Figure 1(b), the Soret band of Mb-AuNPs located at 531 nm. Both the oxazolone (338 nm) and imidazolone (387 nm) rings of Mb were as evidenced by a decrease in absorbance at 338 and 387 nm associated with the oxazolone and imidazolone rings, respectively. Based on the UV-visible absorption spectrum changes following β-mercaptoethylamine (0.05 M) addition of 5 μL, gold nanoparticles appeared to bind to AuNPs as evidenced by a decreased absorbance and had a red shift of 530 nm. While the addition of Mb to mercaptoethylamine-AuNPs showed absorption changed, because of range characteristic of

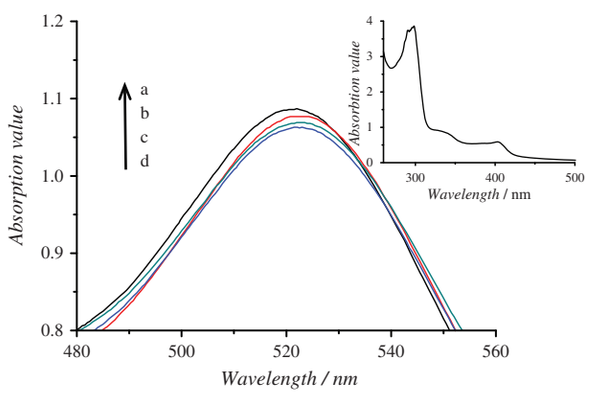

Figure 1. The UV-spectra of pure gold nanoparticles (a), Mb-AuNPs (b), mercaptoethylamine-AuNPs (c), Mb functionalized gold nanoparticles (d). The UV-visible spectra of were measured in a quartz cuvette operated at a resolution of 1 nm from 200 to 800 nm with a high scanning speed. Deionized water was used as blank. The inset was Mb.

metal ligand charge transfer transitions in compounds containing thiol groups (Figs. 1(c, d)).[16–20] This was accompanied by a red shift of the 530 nm maxima to 534 nm with the addition, due to the integration of the plasma of neighboring particles.[21]

3.2. FTIR Spectra

In order to recognize the biological groups that bound to the gold surface, we carried out FTIR measurements. For the sake of comparison, the FTIR analysis was used for the characterization of the freeze-dried Mb (a), Mb-AuNPs (b) and the synthesized AuNPs by a new way (Fig. 2 curve c). As shown in Figure 2(a), the marker bands of Tyr residues, oxazolone and imidazolone framework were observed. We can get the results that some peaks of Mb-AuNPs were decreased largely that was same as the reference, in Figure 2(b).[3,14] Many peaks were still seen in the experiment using the FTIR spectrum of Mb functionalized AuNPs, but they all smaller than those Mb. The absorption peaks of vibration bands of –OH group located at 3430 cm^{-1}. The band at 2928 and 2853 cm^{-1} corresponded to C=O asymmetric and symmetric stretching vibration of $–CH_2$, respectively. Peak at 1630 cm^{-1} can be attributed to the stretching vibrations of C=C. The bands at 1043, 1122, and 1261 cm^{-1} can be assigned to the C–O stretching vibrations. While, the band at 1384 cm^{-1} corresponding to C–N stretching vibrations of aromatic amines tyrosine was the most worthy of attention. In general, the stability of AuNPs mainly depends on the existence of stabilizers, such as stabilizing ligand or polymer. The FTIR revealed that Mb as the surface active molecules acted as stabilization agents capping on the surface of AuNPs. In addition, FTIR revealed that AuNPs were functionalized with biomolecules that had carbonyl groups, –OH groups, and other stabilizing functional groups. On the other hand, the bands at 1384 cm^{-1} corresponding to C–N stretching vibrations of tyrosine were weakened due to the reduction of metal ions.

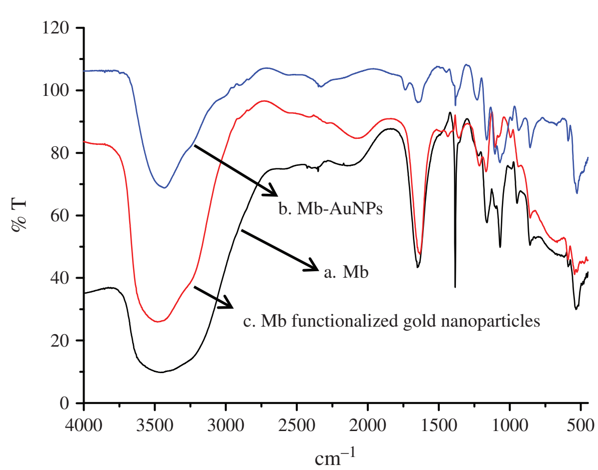

Figure 2. FTIR spectra of Mb (a), Mb-AuNPs (b), Mb functionalized gold nanoparticles (c).

Compared with the Mb-AuNPs, Mb functionalized gold nanoparticles not only had the bioactivity of Mb, but also spatial orientation of Mb on the surface of Au nanoparticles had been better. At the same time, the more $–NH_2$ of the amino residue of the surface of Mb functionalized gold nanoparticles make sure that it can better modified the surface of bare gold electrode by self-assembly.

3.3. Electrochemical Impedance Spectroscopy (EIS)

The information about the impedance changes of the electrode surface in the modification process can be given by EIS. In EIS, the semicircle diameter of EIS equals the electron transfer resistance, R_{ct}. This resistance controls the electron transfer kinetics of the redox-probe at the interface of electrode. There is a very small semicircle domain as was shown in Figure 3(a), which was the EIS of the bare gold electrode. It implied a very low eT resistance ($R_{ct} = 860$) to the redox-probe dissolved in the electrolyte solution. After being added in deaerated Mb aqueous solution, the EIS of the resulting assembled Mb monolayer showed an interfacial eT resistance ($R_{ct} = 1.9 \times 10^3$, Fig. 3, curve b), indicating that the Mb monolayer obstructed eT of the electrochemical probe. Because the AuNPs had larger specific surface area, the Mb-AuNPs monolayer had a higher interfacial eT resistance ($R_{ct} = 4.6 \times 10^3$, Fig. 3, curve c).[7] It may show that on the surface of Mb-AuNPs modified Au gold more Mbs were immobilized. When on the surface of bare gold electrode being added Mb, the EIS of the gold colloid-mercaptoethylamine-modified electrode ($R_{ct} = 6.6 \times 10^3$, Fig. 3, curve d) was smaller than that of the mercaptoethylamine-AuNPs-Mb modified electrode ($R_{ct} = 1.2 \times 10^4$, Fig. 3, curve e). This implied that the Mb was immobilized on the surface of the mercaptoethylamine-AuNPs modified Au electrode. However, as shown in Figure 3(e), the max EIS was for the gold electrode modified with the Mb functionalized gold

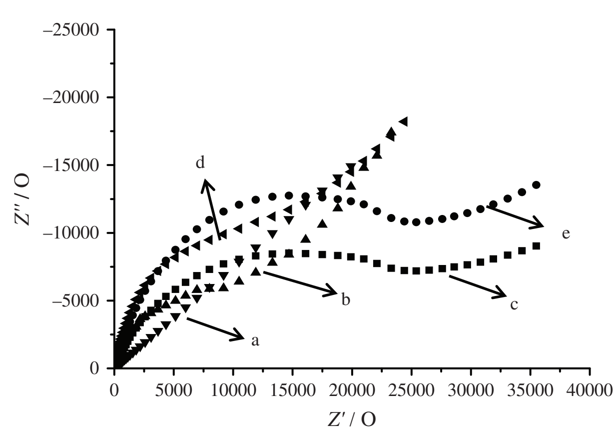

Figure 3. The electrochemical impedance spectroscopy of (a) Bare gold electrode, (b) Mb modified gold electrode, (c) Mb-AuNPs modified gold electrode, (d) mercaptoethylamine-AuNPs modified gold electrode, (e) Mb functionalized gold nanoparticles modified gold electrode.

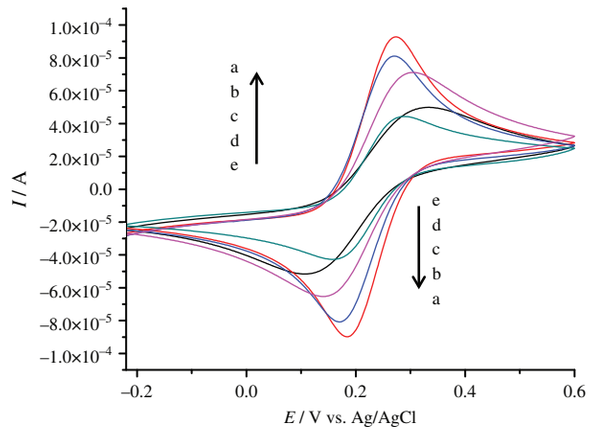

Figure 4. Cyclic voltammograms was obtained by using 0.1 M KCl solution containing 5.00×10^{-3} M $K_3[Fe(CN)_6]$ and 5.00×10^{-3} M $K_4[Fe(CN)_6]$ at a 3 mm diameter gold electrode modified by Mb (a), Mb-AuNPs (b), Mb-AuNPs-mercaptoethylamine (c) and Mb functionalized gold nanoparticles (d) before and after coordination with copper ion, at a scan rate of 100 $mV \cdot s^{-1}$, respectively.

nanoparticles. The reason may be that the certain proportion of thiol reagents and Au nanoparticles can adjust the ratio and spatial orientation of Mb on the surface of Au nanoparticles. This resulted in a denser and more ordered arrangement of Mbs on the surface of Au nanoparticles and more functional materials (Mb) were adsorbed as well, as shown as in Scheme 1(d). Consequently, Mb attached to the gold colloid surface has more spatial freedom in its orientation, making it much easier for the electroactive center of Mb to unfold. As a result, the coverages of electrodes (b to e) were 0.12, 0.21, 0.34 and 0.56, respectively.

Cyclic voltammograms obtained by using 0.1 M KCl solution containing 5.0×10^{-3} M $K_3[Fe(CN)_6]$ and 5.0×10^{-3} M $K_4[Fe(CN)_6]$ showed the same results as the EIS and implied that the surface of the gold electrode modified with Mb functionalized gold nanoparticles had more materials to hinder electrons transport, as shown in Figure 4. On the surface, capacitances per unite area (C_d) of bare gold electrode, Mb (a), Mb-AuNPs (b), Mb-AuNPs-mercaptoethylamine (c) and Mb functionalized gold nanoparticles (d) modified electrode were 160, 147, 129, 43 and 38 $\mu F\ cm^{-2}$, respectively.[22]

3.4. Direct Electrochemistry of Mb and Electrocatalysis of Biosensor to H_2O_2

3.4.1. Cyclic Voltammograms of Copper-Loaded Mbtins Modified Electrodes

Methanobactins and copper-loaded Mbtins exhibit a range of reduction potentials. Shown in Figure 5 are the cyclic voltammograms (CVs) of the Mb (a), Mb-AuNPs (b), mercaptoethylamine-AuNPs-Mb (c) and the Mb functionalized gold nanoparticles (d) modified Au electrode in PBS 64 at 100 mV/s before and after coordination with copper ion, respectively. There was no peak in the CV

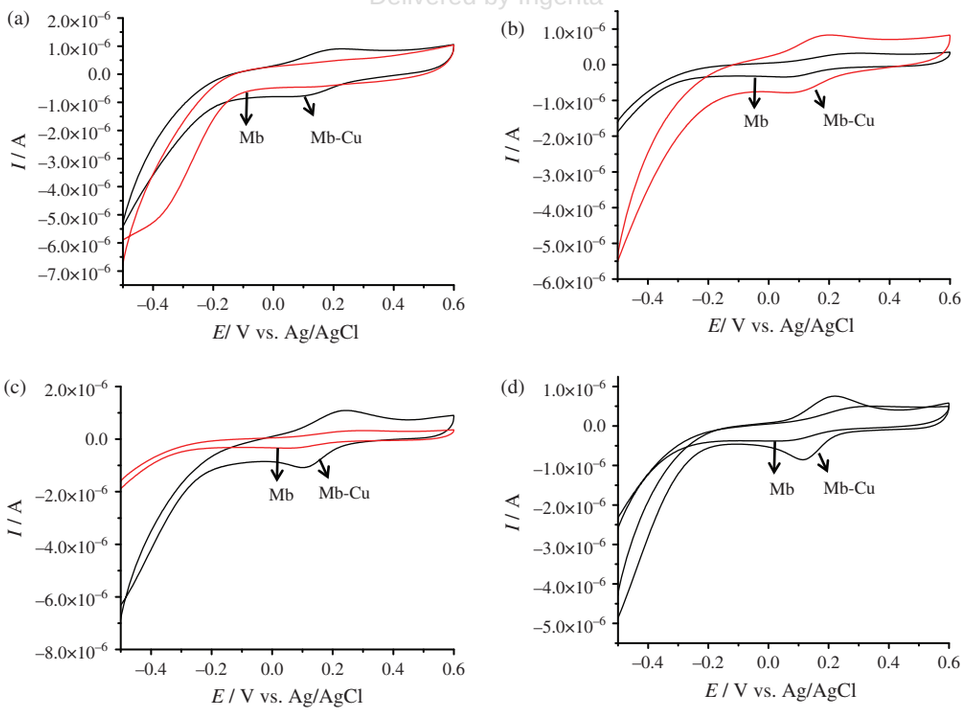

Figure 5. Cyclic voltammograms obtained from pH 6.4 phosphate buffer (0.02 M) at a 3 mm diameter gold electrode modified by Mb (a), Mb-AuNPs (b), Mb-AuNPs-mercaptoethylamine (c) and Mb functionalized gold nanoparticles (d) before and after coordination with copper ion, at a scan rate of 50 $mV \cdot s^{-1}$, respectively.

of a bare Au electrode in such PBS. While in pH 6.4 PBS there was a small peak at the Mb modified Au electrode (Fig. 5(a)). The similar situations happened at the gold electrodes which were modified with Mb-AuNPs, mercaptoethylamine-AuNPs-Mb and Mb functionalized gold nanoparticles, respectively (Figs. 5(b–d)).

However, the copper-loaded Mbtins had higher reduction potentials than Methanobactins. A pair of quasi-reversible redox peaks was observed on modified gold electrode after coordination with copper ion in pH 6.4 PBS that showed that we successfully loaded copper ions onto the surfaces of various modified gold electrodes. After loading of copper ions, the E_0' values of modified electrodes were measured by cyclic voltammetry and were 0.143, 0.170, 0.177 and 0.169 V, respectively (Figs. 5(a–d)). In Figure 5(b), the reduction and oxidation peak potentials of copper-loaded Mbtins were 0.035 and 0.305 V. In Figure 5(c), the *Em* values ranged from 0.11 V to 0.244 V. In Figure 6(d), the reduction and oxidation peak potentials of Au electrode (copper-loaded Mbtins) modified with Mb functionalized gold nanoparticles were 0.115 and 0.222 V, respectively. These results conform with the reference.[23] But these *Em* values are different from the data of other references that are primarily due to the various structures of Mbs and the different affinities of Cu(II). Such variations in copper affinity result in some significant physiological consequences.[24–26]

On one hand, the thiol and amine groups provided by the β-mercaptoethylamine functional groups are assumed to bind irreversibly to the gold electrode surface to give a monolayer peptide coverage. Thus, this form of chemical modification which uses –SH groups of Mb and β-mercaptoethylamine to bind to gold nanoparticles and leaves a surface containing both negative and positive charged sites for binding of bare gold electrode. As a result, it transforms an essentially electroinactive bare gold electrode surface into an electroactive surface.

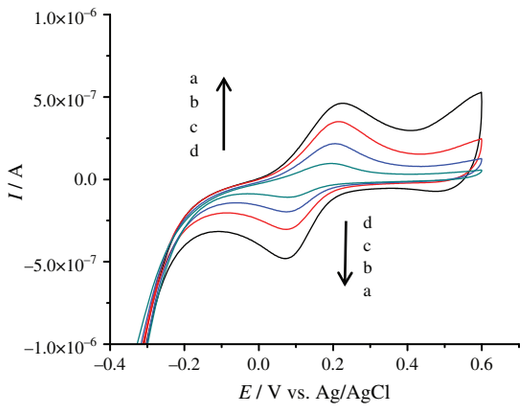

Figure 6. Cyclic voltammograms of a gold electrode modified with Mb functionalized gold nanoparticles in pH 6.4 PBS buffer (0.02 M) at scan rates of (a) 20, (b) 50, (c) 100 and (d) 150 $mV \cdot s^{-1}$.

On the other hand, experimental results showed that the alternating impedance of the Mb-AuNPs, Mb-AuNPs-mercaptoethylamine and Mb functionalized gold nanoparticles modified gold electrode are equivalent to bulk gold electrodes essentially and better than Mb modified gold electrode. The gold colloid nanoparticles makes it easier for the electron transfer to take place, because AuNPs have a high ratio of surface to volume and paly the major role of an efficient electron-conducting tunnel.[27] Thus, it is possible to facilitate and achieve fast direct electron transfer between the loaded-copper Mb and the electrode surface.

3.4.2. The Effection of Different Scan Rates

Then, how the different scan rates affect loaded-copper Mb functionalized gold nanoparticles on the surface of Au electrode was researched. As shown in the CVs, when Cu^{2+} was embedded in the Mb, a pair of redox peaks could be observed. The peak current versus scan rate plots are linear from 20 to 150 $mV \cdot s^{-1}$ (Fig. 6, curves a–d), indicating that this is a surface eT process. The peak-to-peak separation was about ca. 47 mV. As the scan rates were varied from 20 to 150 $mV\ s^{-1}$, the average values of *Em* were 16.5, 17.4 mV, 18.8 mV, and 19.5 mV (vs. Ag/AgCl) respectively.[28]

3.4.3. Amperometric Response of the H_2O_2 Biosensor

In order to observe the activity of loaded-copper Mb at the surface of gold electrode, its response to the reduction of H_2O_2 was studied. And after loading copper ions, Mb functionalized gold nanoparticles had the best reduction of H_2O_2. Figure 7 showed the steady-state current response of H_2O_2. The detection limit of Mb functionalized gold nanoparticles (loaded copper) was 0.9×10^{-5} mA/M (three times as big as the ratio of signal to noise), which was bigger than that of H_2O_2 sensors based on horseradish peroxidase and Hb.[29, 30] But the results effectively proved that the Mb–Cu complexes had peroxidase activity and we successfully prepared a new style of biosensor for determination

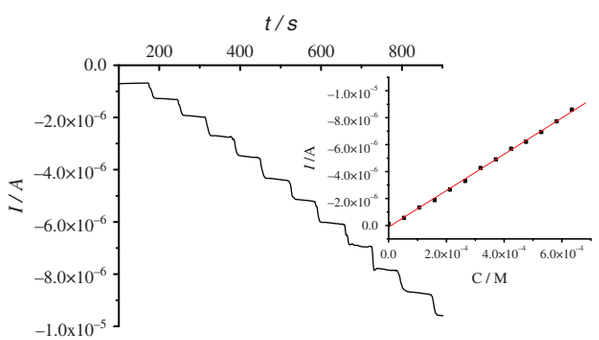

Figure 7. Amperometric response of the H_2O_2 biosensor to successive addition of H_2O_2 0.02 M PBS 6.4 solution at the working potential of −0.2 V. Inset shows the calibration plot between the current and the concentration of H_2O_2. Inset shows the calibration plot between the current and the concentration of H_2O_2.

of H_2O_2 through this study on the modified electrodes method.

Moreover, the response was linear within the concentration range from 5.29×10^{-5} to 6.4×10^{-4} M. The relationship between current and the concentration of H_2O_2 was showed (Fig. 7). According to Lineweaver–Burk equation,[31] the apparent Michaelis–Menten constant K_M^{app} of the H_2O_2 sensor was calculated to be 0.787 mM and low, uggesting that the present sensor exhibits a high affinity for reduction of H_2O_2. The response time was 2 s approximately.

3.5. Stability of the Mb Functionalized Gold Nanoparticles Modified Gold Electrode

If the concentration of H_2O_2 is higher than 5.0×10^{-3} M, the gold electrode modified with the Mb functionalized gold nanoparticles will be denatured. While further studies showed that electrode modified with Mb functionalized gold nanoparticles is very stable. When it was stored in a pH 6.4 PBS for at least 2 weeks at 4 °C, the electrode retained more than 90% of its initial response to the reduction of H_2O_2.

4. CONCLUSIONS

UV-Vis, fluorescence spectra and FTIR spectra can be used to characterize the modified gold nanoparticles, such as Mb functionalized gold nanoparticles and Mb-AuNPs-mercaptoethylamine. The three-dimensional assembly with nanometric Au-colloids achieves the direct electron transfer to Mb and allows us to construct Mb functionalized gold nanoparticles modified gold electrode as a new kind of biosensor for the determination and reduction of H_2O_2. Recently, some novel electrochemical sensors developed with the help of nnaomaterials have been reported,[32–53] our results can bring about some new messages to readers. Moreover, the preparation,[54–69] functionalization,[70–88] and characterization,[89–94] and applications[95–107] have extensively described. We believe gold nanoparticles will find more and more application in biomedical field.[108–110]

Acknowledgments: Financial support by the National Natural Science Foundation of China (grant No. 21573055), the Research Team Support Project of Harbin University of Commerce (grant No. 2016TD006) and the Laboratory of Biocatalysis, Food engineering college, Harbin Commerce University of China are gratefully acknowledged.

References and Notes

1. J. Y. Xin, K. Lin, Y. Wang, and C. G. Xia, *Appl. Biol. Chem.* 58, 1 (**2015**).
2. K. Lin, J. Y. Xin, Y. Wang, Y. Yang, and C. G. Xia, *J. Mol. Catal.* 28, 427 (**2014**).
3. J. Y. Xin, K. Lin, Y. Wang, and C. G. Xia, *J. Mol. Sci.* 15, 21603 (**2014**).
4. J. Y. Xin, L. X. Zhang, D. D. Chen, K. Lin, H. C. Fan, and Y. Wang, *Food Chem.* 174, 473 (**2015**).
5. J. Y. Xin, D. D. Chen, L. X. Zhang, K. Lin, H. C. Fan, Y. Wang, and C. G. Xia, *Int. J. Mol. Sci.* 14, 7226 (**2013**).
6. J. Zhao, R. W. Henkens, J. Stonehuerner, J. P. O'Daly, and A. L. Crumbliss, *J. Electroanal. Chem.* 327, 109 (**1992**).
7. B. X. Dou, J. Y. Xin, H. C. Fan, Y. Wang, and C. G. Xia, *J. Mol. Catal.* 30, 391 (**2016**).
8. H. Y. Gu, A. M. Yu, and H. Y. Chen, *J. Electroanal. Chem.* 516, 119 (**2001**).
9. A. Sassolas, B. D. Lecabouvier, and L. J. Blum, *Chem. Rev.* 108, 109 (**2015**).
10. D. Huang, S. C. Charlton, S. J. George, and A. J. Edelbrock, *Chem. Soc. Rev.* 39, 1747 (**2016**).
11. H. P. Wu, Microdeposition system for a biosensor, U.S. Patent 20160089650 (**2016**).
12. O. D. Velev and E. W. Kaler, *Langmuir* 15, 3693 (**2015**).
13. J. Y. Xin, Y. X. Zhang, J. Dong, Q. Q. Zhou, Y. Wang, X. D. Zhang, and C. G. Xia, *World J. Microbiol. Biotechnol.* 26, 701 (**2010**).
14. L. X. Zhang, J. Y. Xin, D. D. Chen, Y. Wang, and C. G. Xia, *Chem. Eng.* 6, 42 (**2013**).
15. G. Frens, *Nat. Phys. Sci.* 241, 20 (**1973**).
16. M. Vasak, J. H. R. Kaegi, and H. A. O. Hill, *Biochem.* 20, 2852 (**1981**).
17. K. B. Nielson and D. R. Wing, *J. Biol. Chem.* 258, 13063 (**1983**).
18. M. Webb, *Experientia. Suppl.* 34, 313 (**1979**).
19. K. B. Nielson, C. L. Atkin, and D. R. Winge, *J. Biol. Chem.* 260, 5342 (**1985**).
20. G. K. Carson, P. A. W. Dean, and M. J. Stillman, *Inorganica. Chimica. Acta.* 56, 59 (**1985**).
21. M. Quinten, U. Kreibig, D. Schönauer, and L. Genzel, *Surf. Sci.* 156, 741 (**1985**).
22. N. Bandow, V. S. Gilles, B. Freesmeier, J. D. Semrau, B. Krentz, W. Gallagher, M. T. McEllistrem, S. C. Hartsel, D. W. Choi, M. S. Hargrove, T. M. Heard, L. N. Chesner, K. M. Braunreiter, B. V. Cao, M. M. Gavitt, J. Z. Hoopes, J. M. Johnson, E. M. Polster, B. D. Schoenick, A. M. Umlauf, and A. A. DiSpirito, *J. Inorg. Biochem.* 110, 72 (**2012**).
23. A. E. L. Ghazouani, A. Baslé, J. Gray, D. W. Graham, S. J. Firbank, and C. Dennison, *Proc. Nat. Acad. Sci. U.S.A.* 109, 8400 (**2012**).
24. N. J. Robinson and D. R. Winge, *Annu. Rev. Biochem.* 79, 537 (**2010**).
25. L. Banci, I. Bertini, S. Ciofi-Baffoni, T. Kozyreva, K. Zovo, and P. Palumaa, *Nat.* 465, 645 (**2010**).
26. A. Badarau and C. Dennison, *Proc. Nat. Acad. Sci. U.S.A.* 108, 13007 (**2011**).
27. J. Zhao, R. W. Henkens, J. Stonehuerner, J. P. O'Daly, and A. L. Crumbliss, *J. Electroanal. Chem.* 327, 109 (**1992**).
28. J. Li and S. Dong, *J. Electroanal. Chem.* 431, 19 (**1997**).
29. Z. Yan, Z. Yiqun, K. Rongmei, X. Lian, and Q. Fengli, *Biosens. Bioelectron.* 75, 383 (**2016**).
30. Y. Sun, H. Y. Du, Y. T. Lan, W. J. Wang, Y. J. Liang, C. L. Feng, and M. Yang, *Biosens. Bioelectron.* 77, 894 (**2016**).
31. R. A. Kamin and G. S. Wilson, *Anal. Chem.* 52, 1198 (**1980**).
32. N. Wang, H. Dai, D. Wang, L. Chen, H. Ma, and M. Lin, *Nanosci. Nanotechnol. Lett.* 8, 581 (**2016**).
33. K. Krishnamoorthy, G. Veerasubramani, S. Radhakrishnan, and S. J. Kim, *J. Nanosci. Nanotechnol.* 15, 4409 (**2015**).
34. J. Shu, W. Shen, and H. Cui, *Sci. China Chem.* 58, 425 (**2015**).
35. Y. Deng, W. Wang, C. Ma, and Z. Li, *J. Biomed. Nanotechnol.* 9, 1378 (**2013**).
36. C. Cui, H. Wang, X. Zhu, J. Han, and Q. Ge, *Sci. China Chem.* 58, 607 (**2015**).
37. K. Liu, H. Dong, and Y. Deng, *J. Nanosci. Nanotechnol.* 16, 6648 (**2016**).

38. E. Hamidi-Asl, J. B. Raoof, A. S. Meibodi, and Z. H. Bazgir, *Sci. China Chem.* 59, 128 **(2016)**.
39. Y. Liu, Y. Deng, H. Dong, K. Liu, and N. He, *Sci. China Chem.* 60, 329 **(2017)**.
40. S. Han, Z. Zhang, S. Li, L. Qi, and G. Xu, *Sci. China Chem.* 59, 794 **(2016)**.
41. Y. Deng, W. Wang, L. Zhang, Z. Lu, S. Li, and L. Xu, *J. Biomed. Nanotechnol.* 9, 318 **(2013)**.
42. S. S. Low, M. T. T. Tan, P. S. Khiew, H.-S. Loh, and W. S. Chiu, *J. Nanosci. Nanotechnol.* 16, 7420 **(2016)**.
43. Z. Wang, X. Yang, J. Yang, Y. Jiang, and N. He, *Anal. Chim. Acta* 862, 53 **(2015)**.
44. W. Wang, Y. Deng, L. Xu, and X. He, *J. Biomed. Nanotechnol.* 9, 736 **(2013)**.
45. Y. Wang and S. Hu, *J. Nanosci. Nanotechnol.* 16, 7852 **(2016)**.
46. Y. Liu, K. Liu, H. Dong, L. Zhang, Y. Deng, C. Ma, and Z. Wang, *Nanosci. Nanotechnol. Lett.* 8, 785 **(2016)**.
47. Y. Ma, Y. Yu, M. Xu, X. Yan, D. Chen, and M. Ma, *Nanosci. Nanotechnol. Lett.* 8, 592 **(2016)**
48. L. Cao, C. Fang, Y. Liang, X. Zhao, Y. Jiang, and Z. Chen, *J. Nanosci. Nanotechnol.* 16, 12187 **(2016)**.
49. Y. Deng, K. Liu, Y. Liu, H. Dong, and S. Li, *J. Nanosci. Nanotechnol.* 16, 9460 **(2016)**.
50. J. Wang, D. Zhao, and C. Xu, *J. Nanosci. Nanotechnol.* 16, 7145 **(2016)**.
51. Q. Zhu, J. Ma, X. Kang, X. Sun, J. Hu, G. Yang, and B. Han, *Sci. China Chem.* 59, 551 **(2016)**.
52. P. Kanchana, S. Radhakrishnan, M. Navaneethan, M. Arivanandhan, Y. Hayakawa, and C. Sekar, *J. Nanosci. Nanotechnol.* 16, 6185 **(2016)**.
53. H. S. Han, M. S. Ahmed, H. Jeong, and S. Jeon, *J. Nanosci. Nanotechnol.* 16, 333 **(2016)**.
54. J. Zhong, B. Guo, J. Xie, S. Deng, N. Fu, S. Lin, G. Li, Y. Lin, and X. Cai. *Bone Res.* 4, 15036 **(2016)**.
55. H. Yi, F. U. Rehman, C. Zhao, B. Liu, and N. He, *Bone Res.* 4, 16050 **(2016)**.
56. L. Lv, W. Ge, Y. Liu, G. Lai, H. Liu, W. Li, and Y. Zhou. *Bone Res*. 4, 16037 **(2016)**.
57. M. Liu, X. Zeng, C. Ma, H. Yi, Z. Ali, X. Mou, S. Li, Y. Deng, and N. He, *Bone Res*. 4, 17014 **(2017)**.
58. M. R. Rubin and J. M. Patsch, *Bone Res*. 4, 16001 **(2016)**.
59. G. Fernandes and S. Yang, *Bone Res*. 4, 16036 **(2016)**.
60. Y. Osman, A. A. Elrazak, and W. Khater, *J. Biobased Mater. Bioenergy* 10, 119 **(2016)**.
61. A. Góra, D. Pliszka, S. Mukherjee, and S. Ramakrishna, *J. Nanosci. Nanotechnol.* 16, 19 **(2016)**.
62. Z. Xi, R. Huang, Z. Li, N. He, T. Wang, E. Su, and Y. Deng, *ACS Appl. Mater. Interfaces* 7, 11215 **(2015)**.
63. M. Liu, P. Hu, G. Zhang, Y. Zeng, H. Yang, J. Fan, L. Jin, H. Liu, Y. Deng, S. Li, X. Zeng, S. Elingarami, and N. He, *Theranostics* 4, 71 **(2015)**.
64. Y. Zhang, Y. Jia, S. Li, Y. Deng, H. Liu, and N. He, *Sci. Adv. Mater.* 6, 1146 **(2014)**.
65. Z. Xi, B. Zheng, and C. Wang, *Nanosci. Nanotechnol. Lett.* 8, 1061 **(2016)**.
66. B. Zhou, H. Yang, Y. Deng, M. Liu, B. Liu, N. He, and Z. Li, *Sci. China Chem*. 59, 1501 **(2016)**.
67. R. Huang, Z. Xi, and N. He, *Sci. China Chem.* 58, 1122 **(2015)**.
68. S.-C. Roh, J.-H. Choi, and H.-I. Seo, *Nanosci. Nanotechnol. Lett*. 8, 38 **(2016)**.
69. L. Jin, X. Zeng, M. Liu, Y. Deng, and N. He, *Theranostics* 4, 240 **(2014)**.
70. D. M. Findlay and J. S. Kuliwaba, *Bone Res.* 4, 16028 **(2016)**.
71. P. Guo and S. L. Lam, *Signal Transduction and Targeted Therapy* 1, e16028 **(2016)**.
72. J. Yu, Z. Chen, C. Wang, Y. Hu, H. Dong, and Y. Deng, *J. Nanosci. Nanotechnol.* 16, 7069 **(2016)**.
73. Y. Deng, Y. Zhang, H. Jiang, L. Xu, H. Liu, S. Li, and N. He, *J. Biomed. Nanotechnol*. 5, 551 **(2009)**.
74. H. Jiang, X. Zeng, N. He, Y. Deng, G. Lu, and K. Li, *J. Nanosci. Nanotechnol*. 13, 1617 **(2013)**.
75. L. Mao, Z. Lu, N. He, L. Zhang, Y. Deng, and D. Duan, *Sci. China Chem*. 60, 157 **(2017)**.
76. X. Shao, S. Lin, Q. Peng, S. Shi, X. Wei, T. Zhang, and Y. Lin, *Small* 12, 1602770 **(2017)**.
77. H. Chen, Y. Wu, Z. Chen, X. Mou, Z. Li, E. Su, Y. Deng, and N. He, *Nanosci. Nanotechnol. Lett.* 8, 1118 **(2016)**.
78. Z. Qin, S. Yang, Y. Wang, J. Wang, Z. Li, M. Wang, W. Zeng, G. J. Duns, F. He, and X. Luo, *Nanosci. Nanotechnol. Lett*. 8, 1047 **(2016)**.
79. M. A. A. Shah, N. He, Z. Li, Z. Ali, and L. Zhang, *J. Biomed. Nanotechnol*. 10, 2332 **(2014)**.
80. J. Yan, N. Joshee, and S. Liu, *J. Biobased Mater. Bioenergy* 10, 339 **(2016)**.
81. B. Li, X. Mou, Z. Chen, H. Chen, Y. Deng, S. Li, E. Su, L. He, and N. He, *Sci. China Chem.* 60, 4 **(2017)**.
82. F. Li, Z. Wang, Y. Huang, H. Xu, L. He, Y. Deng, X. Zeng, and N. He, *J. Biomed. Nanotechnol.* 11, 1776 **(2015)**.
83. Y. Deng, N. He, X. Li, L. Xu, S. Li, Z. Li, and H. Liu, *Adv. Sci. Lett*. 4, 442 **(2011)**.
84. Y. Huang, K. Xia, N. He, Z. Lu, L. Zhang, Y. Deng, and L. Nie, *Sci. China Chem*. 58, 1759 **(2015)**.
85. X. Mou, T. Li, J. Wang, Z. Ali, Y. Zhang, Z. Chen, Y. Deng, S. Li, E. Su, Q. Jia, N. He, J. Ni, and D. Cui, *J. Biomed. Nanotechnol*. 11, 2057 **(2015)**.
86. T. Li, P. Xiao, A. Khan, Z. Wang, and N. He, *Nanosci. Nanotechnol. Lett.* 9, 895 **(2017)**.
87. S. Guo, Z. Yang, and Y. Gao, *J. Biobased Mater. Bioenergy* 10, 34 **(2016)**.
88. L. Tian, S. Li, H. Liu, Z. Wang, and N. He, *J. Biomed. Nanotechnol*. 5, 511 **(2009)**.
89. L. Tang, S. Zhuang, Q. Lu, S. Lin, P. Li, Y. Liao, and B. Huang, *J. Biobased Mater. Bioenergy* 10, 27 **(2016)**.
90. Y. Fang, P. Liao, S. Li, N. He, Z. Chen, H. Chen, Y. Wu, E. Su, and Z. Wang, *Nanosci. Nanotechnol. Lett*. 9, 650 **(2017)**.
91. Z. Ali, J. Wang, Y. Tang, B. Liu, N. He, and Z. Li, *Biomaterials Science* 5, 57 **(2017)**.
92. P. Wang, J. Yu, Y. Qin, and Z. Su, *J. Biobased Mater. Bioenergy* 10, 229 **(2016)**.
93. R. Dungani, H. P. S. A. Khalil, Md. N. Islam, I. Sumardi, P. Aditiawati, and A. Hadiyane, *J. Biobased Mater. Bioenergy* 10, 258 **(2016)**.
94. Z. Lu, L. Zhang, Y. Deng, S. Li, and N. He, *Nanoscale* 4, 5840 **(2012)**.
95. J. Morita and M. Iwamoto, *J. Biobased Mater. Bioenergy* 10, 151 **(2016)**.
96. Y. Deng, M. Wang, L. Jiang, C. Ma, Z. Xi, X. Li, and N. He, *J. Biomed. Nanotechnol.* 9, 1123 **(2013)**.
97. Y. Tang, B. li, J. Dai, J. Dai, X. Wang, J. Si, Z. Ali, T. Li, and N. He. *J. Biomed. Nanotechnol.* 12, 762 **(2016)**.
98. L. Zhang, K. Xia, Z. Lu, G. Li, J. Chen, Y. Deng, S. Li, F. Zhou, and N. He, *Chem. Mater.* 26, 1794 **(2014)**.
99. L. Zhang, K. Xia, Y.-Y. Bai, Z. Lu, Y. Tang, Y. Deng, J. Chen, W. Qian, H. Shen, Z. Zhang, S. Ju, and N. He, *J. Biomed. Nanotechnol.* 10, 1440 **(2014)**.
100. L. Zhang, Z. Lu, Y. Bai, T. Wang, Z. Wang, J. Chen, Y. Ding, F. Yang, Z. Xiao, S. Ju, J. Zhu, and N. He, *J. Mater. Chem. B* 1, 1289 **(2013)**.
101. J. Wang, P. Lu, J. Yan, Y. Zhang, L. Huang, Z. Ali, B. Liu, Z. Li, and N. He, *J. Biomed. Nanotechnol.* 12, 710 **(2016)**.
102. L. Zhang, Z. Wang, Z. Lu, H. Shen, J. Huang, M. Liu, N. He, and Z. Zhang, *J. Mater. Chem. B* 1, 749 **(2013)**.

103. L. Zhang, Z. Lu, X. Li, Y. Deng, F. Zhang, C. Ma, and N. He, *Polym. Chem.* 3, 1958 **(2012)**.
104. R. Huang, Z. Chen, M. Liu, Y. Deng, S. Li, and N. He, *Sci. China Chem.* 60, 786 **(2017)**.
105. X.-B. Mou, Z. Ali, B. Li, T.-T. Li, H. Yi, H.-M. Dong, N.-Y. He, Y. Deng, and X. Zeng, *Chinese Chemical Letters* 27, 1661 **(2016)**.
106. Z. Li, B. Fei, and Z. Jiang, *J. Biobased Mater. Bioenergy* 10, 71 **(2016)**.
107. X. Li, L. Wang, Z. Liang, and J. Wu, *Nanosci. Nanotechnol. Lett.* 8, 1135 **(2016)**.
108. S. Li, H. Liu, Y. Jia, Y. Deng, L. Zhang, Z. Lu, and N. He, *Theranostics* 2, 967 **(2012)**.
109. H. Jiang, X. Zeng, N. He, Y. Deng, G. Lu, and K. Li, *J. Nanosci. Nanotechnol.* 13, 1617 **(2013)**.
110. H. Liu, S. Li, L. Liu, L. Tian, and N. He, *Biosens. Bioelectron.* 26, 1442 **(2010)**.

Received: 27 May 2017. Accepted: 14 July 2017.